Infrared imaging of the surface temperature field of water during film spreading

J. R. Saylor and G. B. Smith
Naval Research Laboratory, Washington, DC 20375

K. A. Flack
United States Naval Academy, Annapolis, Maryland 21402

(Received 4 May 1999; accepted 1 December 1999)

Deposition of a spontaneously-spreading film on a clean water surface creates a front which propagates radially outward from the point of deposition. This rapidly spreading film was used as a tool to quickly change the boundary condition of a water surface from one which is shear-free, to a boundary condition which supports shear. Infrared images of a water surface experiencing evaporative convection were recorded as this film spread. These images were converted to surface temperature fields. The amount of turbulent structure present in these fields changes dramatically across the front. Ahead of the front, significant variations at large and small spatial scales are evident, while behind the front the small scale structures are eliminated. The time scale at which this damping occurs is short and has not been reported on heretofore. In addition to being relevant to free surface turbulence, these results demonstrate the utility of infrared imaging in the study of spreading films. [S1070-6631(00)02703-3]

I. INTRODUCTION

The hydrodynamic boundary condition which exists at a perfectly clean gas/liquid interface is considered to be shear-free. Films, such as surfactant monolayers or liquid-phase multilayers, can support a shear, changing this free surface boundary condition and concomitantly affecting the subsurface hydrodynamics. This alteration in subsurface hydrodynamics can in turn change the surface temperature field, a quantity which is relevant to several oceanographic, meteorological and remote sensing applications, and is the object of interest in this study.

We note that, in addition to influencing subsurface hydrodynamics, some surfactant monolayers can reduce the rate of evaporation,[1,2] thereby affecting the surface temperature field. This effect is not the focus of the work presented herein.

Experimental studies have demonstrated that surface temperature time traces can be significantly affected by the presence of a film.[3–7] Such studies are typically conducted in a water tank where evaporation at the air/water interface cools the water surface, creating an instability which drives natural convection. This evaporatively driven natural convection, referred to as evaporative convection,[8] is typically turbulent. These studies have shown that the average and fluctuating components of the surface temperature, measured at a point, are significantly altered by the presence of a surfactant monolayer.

Further information on the effect that films have on the surface temperature during evaporative convection was obtained in a more recent study where infrared imaging was utilized to measure the surface temperature field.[9] These experiments showed that the small scale turbulent structures evident in the temperature field of a clean water surface were essentially eliminated upon introduction of a surfactant monolayer, leaving only large scale structures. In that work we demonstrated the effect that films have on the surface temperature field under steady state conditions; the transient behavior of this field has not been investigated. In the experiments presented here, a rapidly spreading film was used as a tool to quickly change the boundary condition of a water surface from one which is shear-free, to a boundary condition which supports shear. By measuring the temperature field during the spreading process, information was obtained concerning the speed with which small scale structures in the temperature field were eliminated. In addition to its relevance to free surface turbulence, the spreading of films finds application in the area of oil slicks and their dispersal,[10] the transport of surfactants within the lung,[11] and the formation of Langmuir–Blodgett films.[12]

II. EXPERIMENTAL METHOD

The experiments were conducted in a 30 cm by 30 cm tank having a depth of 15 cm. The tank was filled to the rim with deionized water, and several cleaning steps were used to eliminate any possible contamination from indigenous surfactants.[9] Evaporation from the water surface into the ambient air environment resulted in a heat flux of $\sim 30\ \mathrm{W/m^2}$. The surface temperature field was measured by imaging the surface of the water using an infrared camera. This camera was calibrated, and the calibration was used to convert each infrared image to a temperature field. The optical depth of the infrared camera was ~ 25 microns; hence the fields obtained are maps of the temperature averaged over the top 25 μm of the water depth. We assume our measurements to be representative of the surface temperature, and refer to the measured temperature fields as the 'surface temperature

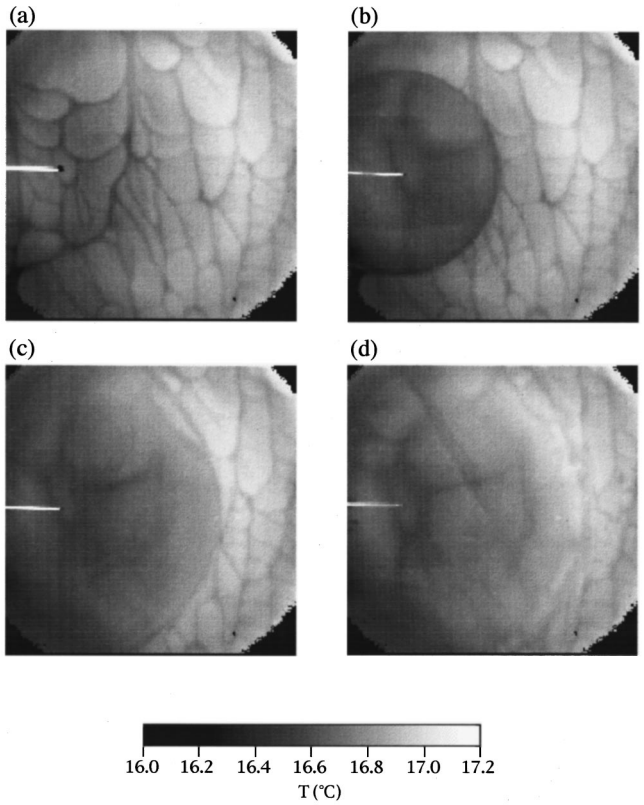

FIG. 1. A sequence of four temperature fields illustrating the spread of a heptane/oleyl alcohol film across a water surface. The time corresponding to each image is (a) 0 ms (b) 250 ms (c) 500 ms, and (d) 750 ms. The size of a pixel in physical space is 635 μm in each direction, giving an image width of 16.1 cm.

field.' The total range in temperature displayed in the temperature fields were on the order of ~ 0.6 K, and the camera had a noise level of approximately 25 mK. The width of the region corresponding to each field was 16.1 cm. Further details of the experimental setup can be found in Saylor *et al.*[9]

To switch the surface boundary condition from shear-free to one that supports shear, a surfactant was deposited on the water surface. This deposition process was recorded by the infrared camera. The surfactant used was oleyl alcohol, which was dissolved in heptane at a concentration of 1.0 mg/ml. A 5 μl drop of this solution was placed on the water surface using a micrometer syringe. The mixture spread over the water surface, resulting in an oleyl alcohol surface concentration of $0.0056\,\mu\text{g/cm}^2$ after evaporation of the heptane. This procedure of dissolving a surfactant in a volatile solvent, prior to deposition, is a standard method used when studying surfactant monolayers. To ensure that the results obtained were not due to the presence of the heptane, which was in the process of evaporating when images were obtained, tests were conducted while applying only pure oleyl alcohol to the water surface. Infrared images obtained during these tests were qualitatively the same as those presented below.

III. RESULTS

A sequence of temperature fields is presented in Figs. 1(a)–1(d) showing the deposition and spreading of the oleyl alcohol/heptane mixture. The separation time between each image in the sequence is 250 ms. A palette indicating the relationship between the gray level in the image and the temperature to which it corresponds, is located at the bottom of the figure. The micrometer syringe used to place the heptane/oleyl alcohol droplet on the water surface is visible in the left hand side of each image. The dark black circle at the tip of the syringe, visible in Fig. 1(a), is the pendant droplet of the mixture which is about to be deposited.

In each image obtained by the camera, some of the pixels located in the corners of the detector gave erroneous responses and were designated ''bad pixels.'' These are the black regions located in the corners of each field, which should be ignored. It should also be noted that the gray scale values of the pixels corresponding to the micrometer syringe cannot be converted to an accurate temperature using the palette included beneath the figure, since the calibration used assumes the emissivity of the imaged region is that of water.

Figure 1(a) shows the temperature field prior to deposition of the film: a clean water surface undergoing evaporative convection. The temperature field exhibits cellular regions of relatively warm fluid (light regions), surrounded by thin regions of relatively cold fluid (dark regions). This pattern is characteristic of that which is observed during infrared imaging of evaporative convection (e.g., Saylor *et al.*).[9] Utilizing simultaneous infrared imaging of the water surface, and subsurface velocity measurements, Volino and Smith[13] demonstrated that these cellular regions are the surface signatures of convective cells, with the cold striated regions corresponding to falling sheets of fluid, and the warm regions in between the sheets corresponding to rising plumes. Katsaros *et al.*[14] observed these falling sheets when obtaining horizontal temperature profiles coupled with flow visualization, beneath a water surface; a review of the literature concerning these convective structures can also be found in Katsaros *et al.*[14]

Figures 1(b)–1(d) show how the cellular pattern of the clean water surface is altered by the spreading film. In Fig. 1(b) the film has spread circularly outward from the point of deposition, and a clearly defined front exists between the clean surface and the spreading film. The circular region is slightly cooler than the rest of the surface and, more importantly, the cellular structures so evident in Fig. 1(a) have been completely damped out in the region behind the front. Actually, there is some thermal structure which remains behind the front but these are very weak and larger in scale than those which exist ahead of the front. The small scale structures which are eliminated by the spreading film do not return. Images obtained over a minute after deposition reveal a surface temperature field which has changed negligibly from that which exists behind the front in Fig. 1. The faint halo which is visible ahead of the front in Fig. 1(b) is believed to be a capillary wave formed at the moment of deposition. In Figs. 1(c) and 1(d), the film continues to spread, and the cellular structures continue to be eliminated in the areas over which the front has passed. In Fig. 1(d), the front is more difficult to see. It appears to exhibit an instability, giving it a ''corrugated'' shape.

It is important to note that the elimination of small scale

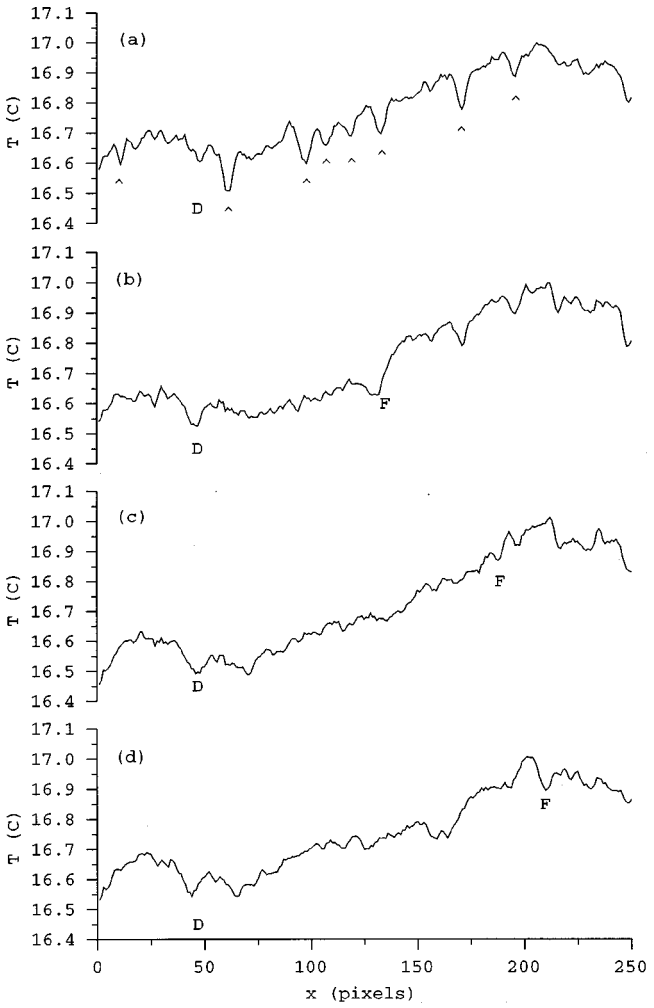

FIG. 2. Line sections of the temperature through the center of each field in Fig. 1. To avoid the micrometer syringe, the line section is actually for row number 132 which is six pixels (3.79 mm) beneath the true centerline. Each line section has been smoothed using a 3 pixel window. ''F'' indicates the location of the front, and ''D'' indicates the deposition location. In (a), ''∧'' indicates the location of the black striated regions.

structures in the surface temperature field does not necessarily signify a change in the subsurface hydrodynamics, although such a change most likely does occur. The measurements presented in Fig. 1 are only temperature fields, and subsurface velocity measurements would be needed to conclusively demonstrate that the change in the surface temperature field is due to a change in subsurface hydrodynamics. This point will be revisited.

Horizontal line sections corresponding to the center of each field presented in Fig. 1 are displayed in Fig. 2. All of these line sections reveal a general left-to-right increase in temperature. This is true even in Fig. 2(a) where the drop has not yet been deposited on the water surface. Careful observation reveals this in Fig. 1(a) as well, where the left hand side of the field appears, on average, to be slightly darker than the right hand side. It is unclear what caused this gradual variation in temperature across the field. This may have been due to a slight variation in the sensitivity of the camera across the image, or it may have been caused by a variation in the cooling of the surface due to air currents in the room, for example.

A comparison of the line sections in Figs. 2(b)–2(d) with the line section in Fig. 2(a) (where the film has not yet been deposited) reveals a slight lowering of the temperature in the region behind the front. This reduction in temperature was computed by averaging the temperature in that portion of the line section located behind the front (using a method for locating the front which is described below) and subtracting this value from an average of the same portion of the line section in Fig. 2(a). This procedure gives a value of $-0.06\,^{\circ}\mathrm{C}$, $-0.08\,^{\circ}\mathrm{C}$, and $-0.03\,^{\circ}\mathrm{C}$ for Figs. 2(b), 2(c), and 2(d), respectively. This reduction in temperature is not due to the general left-to-right variation in temperature, discussed above, since this variation is accounted for when subtracting the two computed averages. This drop in temperature is partly due to evaporation of heptane in the spreading film. O'Brien *et al.*[15] shows a cooling of the surface during the spread of a nonevaporating film which they attribute to an increase in the water evaporation rate due to stirring of the air above the water surface. This may also be playing a role in cooling the region behind the front.

The dark striated regions which surround the convective cells in the area ahead of the front correspond to downward dips in the temperature which can be seen in the plots of Fig. 2. They are particularly evident in Fig. 2(a) and their location is indicated using the ''∧'' symbol. In Figs. 2(b)–2(d) the region behind the spreading front shows an elimination of the downward spikes which are present in Fig. 2(a). This observation agrees with the reduction in the small scale striated structure behind the front seen in Fig. 1.

While the location of the front is easy to spot with the eye in Fig. 1, its exact location is not at all apparent in the line sections of Fig. 2. The lack of downward spikes behind the front does not provide a good measure of the front location, since the distance between the dark striated regions is large relative to the apparent thickness of the front. The fact that the area behind the front has a slightly lower temperature is also difficult to use in locating the front, since the overall variation in temperature across the image is larger than the temperature decrease due to the spreading film, making it difficult to select a temperature threshold which would define the front.

To more rigorously define a front location, a small portion of the temperature field encompassing the front was extracted, thereby making the variation in temperature across the front large with respect to the temperature variation in the subimage. The pdf of the subimages for Figs. 1(b) and 1(c) were bimodal and the minimum between the two peaks was used as a threshold to create a binary image. Figure 3 presents the subimage extracted from Fig. 1(b), as well as the pdf for that subimage and the resulting binary image obtained by setting the threshold to $16.75\,^{\circ}\mathrm{C}$, the temperature corresponding to the minimum between the two peaks of the pdf. The frontal location is obvious in the binary image. The subimage extracted from Fig. 1(d) did not display a bimodal pdf, and instead the front was located by progressively increasing the contrast until the subimage became binary.

The frontal locations calculated in the manner described

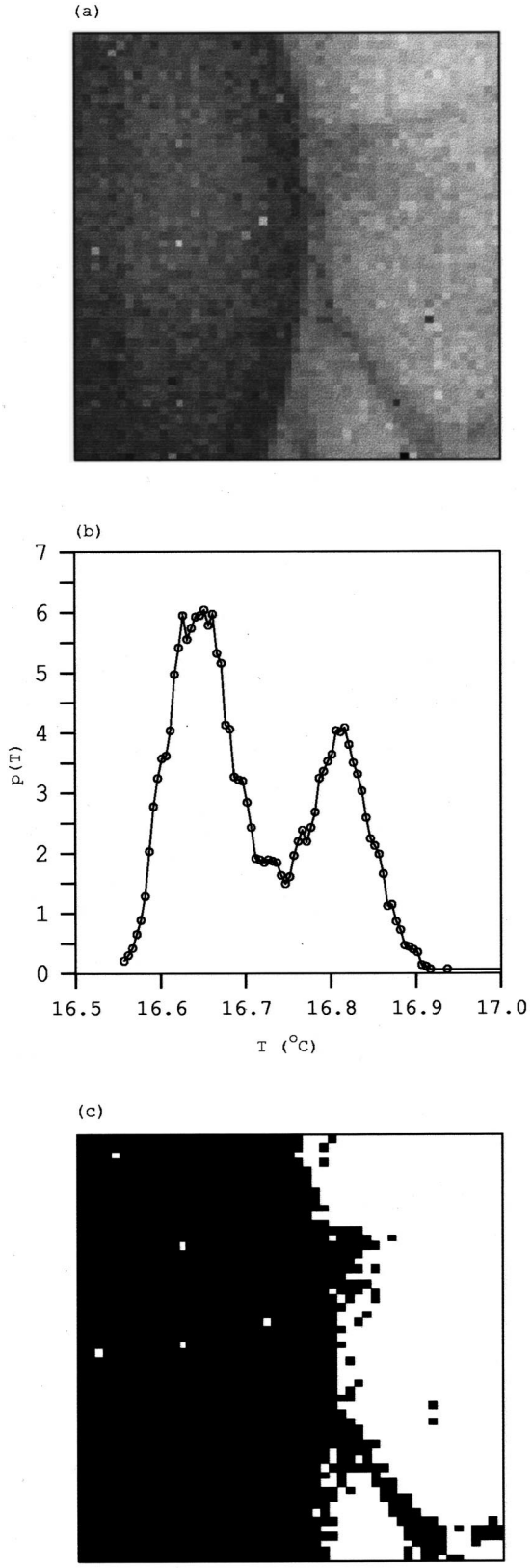

FIG. 3. (a) Subimage extracted from Fig. 1(b). (b) Temperature pdf for the extracted subimage. (c) Binary version of the subimage, obtained by setting a threshold at the minimum between the peaks in the bimodal pdf.

above are catalogued in Table I for Figs. 1(b)–1(d). The droplet deposition location is indicated, along with the x-location of the front for each of the three images. The tabulated frontal locations are signified by the letter ''F'' in Fig. 2.

TABLE I. Location of spreading front.

	Time (ms)	x (pixels)	x (mm)
Drop deposition location		47	29.8
Front in Fig. 1(b)	250	135	85.7
Front in Fig. 1(c)	500	189	120
Front in Fig. 1(d)	750	210	133

Two spreading velocities can be computed from the frontal locations: one from the change in frontal position which occurs between Fig. 1(b) and Fig. 1(c), and one from the change in frontal position which occurs between Fig. 1(c) and Fig. 1(d). The average spreading velocity from Figs. 1(b)–1(c) is 137 mm/s, and from Figs. 1(c)–1(d) it is 52 mm/s. Because the drop has not yet touched the water surface in Fig. 1(a), a spreading rate cannot be computed from Figs. 1(a) and 1(b). O'Brien *et al.*[15] obtained velocity profiles for a spreading film of oleic acid, and reported a surface velocity of 160 mm/s and 80 mm/s at 125 ms and 500 ms after deposition, respectively. While their surfactant differs from the oleyl alcohol/heptane system presented here, it is worthwhile noting that their velocities are in rough agreement with those measured here.

IV. DISCUSSION

An important result is the rate at which a small scale structure in the temperature field is damped. In the 250 ms which elapse between Fig. 1(a) and 1(b), the small scale structures behind the advancing front have been completely eliminated from the temperature field. Note that even in the region just behind the advancing front, no remnant of the original structures are visible. This suggests that the damping occurs rapidly with respect to the speed at which the front propagates. Therefore, an estimate of the time scale τ_d at which these structures are damped can be obtained by dividing the width of the front x_f by the speed at which it propagates, v_f,

$$\tau_d = \frac{x_f}{v_f}. \tag{1}$$

The width of the front is estimated using Fig. 3(a) which shows that the change from the relatively cooler region of the film to the warmer nonfilm region occurs over a distance roughly 5 pixels thick ($\sim$3 mm). Using $x_f = 3$ mm, and $v_f = 137$ mm/s (above), and substituting these values into Eq. (1) gives $\tau_d \sim 22$ ms.

A discussion of the mechanisms which might contribute to the damping of small scale structures in the temperature field is now presented.

It has been established that the structures observed in the surface temperature field during evaporative convection are correlated to the subsurface hydrodynamics.[7,13] Also, it is well known that surface films damp subsurface motion. Hence, it is logical to expect that the damping of a small scale structure evident in Fig. 1 is due to a modification of

the subsurface hydrodynamics, caused by the film. Before discussing this hypothesis, however, several simpler explanations, which concern the blockage of evaporation or infrared radiation by the film, are addressed and discounted.

One might suspect that the elimination of small scale structures behind the front is due to a blockage of infrared emission from the water layer beneath. This is unlikely for several reasons. First, in the instance where there is still heptane present in the layer, its maximum thickness is equal to the droplet volume divided by the area over which the droplet has spread. In Fig. 1(b), this thickness is ~ 0.5 μm. For a layer of this thickness the total attenuation of radiation at the infrared wavelengths used to obtain these fields is insignificant. Furthermore, it is known that deposition of a small drop of a volatile film results in the formation of a small ''reservoir'' at the deposition site, from which the thin liquid film spreads radially outward.[16] Hence, the heptane film can be expected to be even thinner than the calculated 0.5 μm thickness, further reducing any attenuation of infrared emission from the water beneath it. In the event that the heptane has rapidly evaporated, leaving only a monolayer of oleyl alcohol, prior research has demonstrated that infrared emission is insignificantly affected by the presence of a monomolecular film.[17] Finally, the thermal structures which have been eliminated by the advancing film are small in size, while the larger structures have been reduced in their intensity, but are still visible. This observation cannot be explained by optical damping, which would be scale-insensitive.

Another possible explanation for the reduction in small scale structure observed in Fig. 1 is that the evaporation of water is reduced by the presence of the heptane film, thereby reducing evaporative convection. If this were the case, the temperature behind the front would increase. In fact, the mean surface temperature behind the front actually decreases very slightly, suggesting that evaporation reduction is not the cause of the observed behavior. A related possibility is that the heptane has rapidly and completely evaporated, leaving a monolayer of oleyl alcohol which might be stopping evaporation. However, oleyl alcohol has been shown to insignificantly affect evaporation,[7] again obviating the possibility that the small scale damping is due to a reduction in evaporation.

Finally, it is possible that evaporation of heptane has actually increased the heat flux behind the front. All other things held constant, an increase in heat flux would result in more small scale structure in the surface temperature field. The fact that the region behind the front has a *reduced* level of structure indicates that either (i) the heat flux has not increased, or (ii) the heat flux has increased, and the damping due to the surfactant is so effective that the small scale structures are still damped. In either case, it is safe to conclude that a change in heat flux is not the dominant cause of the reduction in small scale structure behind the front.

Having discounted mechanisms which concern the blockage of evaporation or infrared radiation by the spreading film, we now present several physical processes concerning the modification of subsurface hydrodynamics by the film, which may explain the experimental results.

As noted earlier, it is well known that a film damps subsurface fluid motion. A possible explanation of the observed damping of a small scale structure in the surface temperature field is that the spreading film is damping fluid motion in a thin layer of water, preventing the convective structures in the liquid bulk from expressing a thermal signature at the free surface. The camera used in these experiments collects infrared radiation from a layer of water, 25 μm in thickness. For the aforementioned mechanism to be plausible, it is necessary that fluid motion in this 25 μm thick layer be damped and that existing thermal structures homogenize via conduction, in a time scale which is comparable to the observed damping time scale, $\tau_d \sim 22$ ms [Eq. (1)]. The time scales for this viscous damping and thermal homogenization are τ_v and τ_t, respectively, and are estimated as

$$\tau_v = \frac{L^2}{\nu} \tag{2}$$

and

$$\tau_t = \frac{L^2}{\alpha}, \tag{3}$$

where ν is the kinematic viscosity of liquid water and α is the thermal diffusivity. Substituting 25 μm for L in each equation gives $\tau_v = 0.6$ ms and $\tau_v = 4$ ms, the sum of which is less than $\tau_d = 22$ ms. This suggests that the damping of subsurface motion and the subsequent homogenization of existing thermal structures in a 25 μm thick layer of water can occur within the observed 22 ms damping rate. This is a crude estimate, and a closer agreement between τ_d and the sum of τ_v and τ_t is not expected. This analysis does not prove that the experimental results are caused by this mechanism, but only that this mechanism can explain what was observed.

Another possible explanation for the rapid elimination of small scale structures is that these structures are being smeared as the film rapidly advances across the surface. As the film advances, some liquid may be entrained, effectively being ''pulled'' by the spreading film and smearing out the structures. There is some support for this idea in the imagery. For example, referring to Fig. 1(a), there is a circular structure apparent in the field located just beneath the tip of the micrometer syringe. In Fig. 1(b), this structure has become larger, suggesting that it has been radially stretched by the moving film. However, the effectiveness of the damping seems to be the same as the film progresses outward, where its velocity is lower and one would expect a reduction in the effect. Hence, while this mechanism may be playing a role in what is observed other effects are probably dominant.

The work of Dussaud *et al.*[18] provides another possible mechanism. In this work, it is demonstrated that the spreading of a volatile liquid film on a water surface creates a vortex roll which propagates radially outward, just behind the spreading film and just beneath the air/water interface. If such a vortex is present in our experiments, then it would be logical to assume that it homogenizes the surface temperature field by mixing the surface fluid with that just beneath the surface. The strength of this vortex should be expected to

decrease as the film spreads radially, and decreases in velocity. If this is the case, it would seem that the amount of homogenization of the small scale structures should decrease as the film spreads outward, a trend which is not observed, at least for the time interval of the imagery presented in Fig. 1.

It is not possible to state conclusively which of the three mechanisms described above is responsible for the small scale damping observed in these experiments. It is noted that elimination of the small scale structures due to vortex rollup or due to smearing of the surface would result in a reappearance of the small scale structures after the spreading process is complete. This is not the case; the small scale structures never reappear in the infrared imagery once the film has spread. This suggests that while smearing and vortex rollup may be playing a role, the dominant mechanism is most likely attributable to a damping of subsurface motion by the spreading film. It is not possible to state this conclusively, however, and a detailed program of simultaneous infrared and subsurface velocity measurements would be required to connect the observed change in the temperature field with the hydrodynamics.

In addition to their relevance to turbulence near a free surface, the results presented here demonstrate the utility of infrared imaging as a diagnostic tool for measuring the spreading rates of surfactants and thin liquid films. Current methods for performing these measurements can be classified as invasive or noninvasive. Invasive methods, such as those which use teflon particles to track the front,[19] are subject to contamination. Noninvasive methods employ shadowgraphy,[20] where regions of the air/liquid interface which exhibit a finite curvature are visualized. Because a propagating film deforms the air/liquid interface, such shadowgraphic methods can be used to intuit the location of the film front. A drawback of these methods, however, is that the actual location of the film is not detected, since regions of high curvature may not necessarily correspond to the actual location of the film front. Moreover, as the velocity of the film front decreases, the curvature imparted on the surface by the front weakens, reducing the image contrast.

If the elimination of small scale structures in the imagery is due to damping of subsurface turbulence, as postulated, then the infrared imaging method described here represents an improvement over existing methods for studying film spreading. The surface boundary condition changes from shear-free to one which supports shear, *only* at locations covered by the film. If it is indeed this change in boundary condition which changes the infrared image appearance, then the location of the film front can be obtained without ambiguity. Furthermore, since the contrast in the image is due to the damping of these structures, and not the speed at which the front propagates, there is the potential for measuring very slow spreading rates. Furthermore, even well executed shadowgraphic experiments[16,18] show that the contrast at the measured front is not especially sharp, even when the front velocity is relatively high. The unoptimized infrared images presented in this study show a very clear frontal boundary, and further development of the technique can be expected to result in even better contrast.

ACKNOWLEDGMENTS

The authors thank R. A. Handler for suggesting this paper, and G. M. Korenowski and R. I. Leighton for insightful discussions. This work was supported by the Office of Naval Research, through the Naval Research Laboratory and the United States Naval Academy.

[1] V. K. La Mer, in *Retardation of Evaporation by Monolayers: Transport Processes* (Academic, New York, 1962).
[2] G. T. Barnes, ''The effects of monolayers on the evaporation of liquids,'' Adv. Colloid Interface Sci. **25**, 89 (1986).
[3] U. Navon and J. B. Fenn, ''Interfacial mass and heat transfer during evaporation: I. An experimental technique and some results with a clean water surface,'' AIChE. J. **17**, 131 (1971).
[4] U. Navon and J. B. Fenn, ''Interfacial mass and heat transfer during evaporation: II. Effect of monomolecular films on natural convection in water,'' AIChE. J. **17**, 137 (1971).
[5] N. L. Jarvis, ''The effect of monomolecular films on surface temperature and convective motion at the water/air interface,'' J. Colloid Sci. **17**, 512 (1962).
[6] N. L. Jarvis, C. O. Timmons, and W. A. Zisman, ''The effect of monomolecular films on the surface temperature of water,'' in *Retardation of Evaporation by Monolayers*, edited by V. K. La Mer (Academic, New York, 1962), pp. 41–58.
[7] K. B. Katsaros and W. D. Garrett, ''Effects of organic surface films on evaporation and thermal structure of water in free and forced convection,'' Int. J. Heat Mass Transf. **25**, 1661 (1982).
[8] J. C. Berg, A. Acrivos, and M. Boudart, ''Evaporative convection,'' in *Advances in Chemical Engineering*, edited by T. B. Drew, J. W. Hoopes, T. Vermeulen, and G. R. Cokelet (Academic, New York, 1966), pp. 61–124.
[9] J. R. Saylor, G. B. Smith, and K. A. Flack, ''The effect of a surfactant monolayer on the temperature field of a water surface undergoing evaporation,'' Int. J. Heat Mass Transf. **43** (2000).
[10] D. P. Hoult, ''Oil spreading on the sea,'' Annu. Rev. Fluid Mech. **4**, 341 (1972).
[11] J. B. Grother, ''Pulmonary flow and transport,'' Annu. Rev. Fluid Mech. **26**, 529 (1994).
[12] M. C. Petty, *Langmuir–Blodgett films: An Introduction* (Cambridge University Press, Cambridge, MA, 1996).
[13] R. J. Volino and G. B. Smith, ''Use of simultaneous IR temperature measurements and DPIV to investigate thermal plumes in a thick layer cooled from above,'' Exp. Fluids **27**, 70 (1999).
[14] K. B. Katsaros, W. T. Liu, J. A. Businger, and J. E. Tillman, ''Heat transport and thermal structure in the interfacial boundary layer measured in an open tank of water in turbulent free convection,'' J. Fluid Mech. **83**, 311 (1977).
[15] R. N. O'Brien, A. I. Feher, and J. Leja, ''Interferometric and hydrodynamic flow profiles produced in water by a spreading monolayer,'' J. Colloid Interface Sci. **51**, 366 (1975).
[16] A. D. Dussaud and S. M. Troian, ''Dynamics of spontaneous spreading with evaporation on a deep fluid layer,'' Phys. Fluids **10**, 23 (1998).
[17] N. L. Jarvis and R. E. Kagarise, ''Determination of the surface temperature of water during evaporation studies. A comparison of thermistor with infrared radiometer measurements,'' J. Colloid Sci. **17**, 501 (1962).
[18] A. D. Dussaud, S. M. Troian, and S. R. Harris, ''Fluorescence visualization of a convective instability which modulates the spreading of volatile surface films,'' Phys. Fluids **10**, 1588 (1998).
[19] D. W. Camp and J. C. Berg, ''The spreading of oil on water in the surface tension regime,'' J. Fluid Mech. **184**, 445 (1987).
[20] W. Merzkirch, ''Density sensitive flow visualization, in *Methods of Experimental Physics*, No. 18 in Fluid Dynamics, edited by R. J. Emrich (Academic, New York, 1981), Chap. 2, pp. 345–402.